行政院國家科學委員會專題研究計畫　期中進度報告

以網路模型探討布朗膠體在過濾器中的過濾行為(2/3)

計畫類別：個別型計畫
計畫編號：NSC94-2214-E-029-003-
執行期間：94 年 08 月 01 日至 95 年 07 月 31 日
執行單位：東海大學化學工程學系

計畫主持人：張有義

報告類型：精簡報告
報告附件：出席國際會議研究心得報告及發表論文
處理方式：本計畫可公開查詢

中　華　民　國 95 年 3 月 29 日

期中精簡報告

以網路模型探討布朗膠體在過濾中的過濾行為(2/3)

NSC 94-2214-E-029-003

張有義教授

台中市東海大學化工系

Abstract

The track of individual particles moving through a filter bed is simulated by applying the Brownian dynamics simulation method and the modified square network model. The effect of the Raleigh type size distribution of particles and of pores on the permeability reduction of porous media is also investigated. We find that the pore size distribution of porous media has more profound effect on the reducing of the permeability ratio than that of the particle size distribution especially at the initial period of filtration. Straining is the main mechanism to reduce the permeability at the initial period of injection for the case of Raleigh distribution of the pore size, and vice versa for the case of unique size value where the direct deposition mechanism becomes dominant.

Email:yichang@thu.edu.tw Fax:00-886-4-23590009

1. Introduction

Deep bed filtration is a process involving the transport and deposition of colloidal particles within the porous media. During the course of filtration, the accumulation of deposited particles increases with time until the breakthrough moment is achieved. Consequently, those deposited particles reduce the permeability of the filter (Tien, 1989). The permeability reduction rate along the filter bed is dependent on several system parameters which has been the subjects of numerous studies, those parameters are: the fluid superficial velocity, the grain and particle sizes (Ison and Ives, 1969; Herzig, Leclerc and Goff, 1970; Yao, 1972), the geometry of collector (Tien and Payatakes, 1979), the interaction forces between particles and collector surfaces (Kim and Rajagopalan, 1982; Chang and Whang, 1998), and the pore size distribution (Sharma and Yortsos, 1987; Rege and Fogler, 1988; Imdakm and Sahimi, 1991; Chang et al., 2004).

In our previous paper (Chang et al., 2004), with the adoption of the Brownian dynamic simulation method and the constricted tube model representing the geometry of porous media (see Fig. 1), we had successfully applied the two-dimensional modified square network model to track the individual particles with Brownian motion behavior as they move through the filter bed (i.e. the Langevin type approach). From which, caused either by the straining or by the direct deposition of particles on the pore walls, the temporal variations of the permeability reduction and the pressure drop were successfully determined. More important, we found that the permeability decreases significantly when the size distributions of particles and pores are both considered. But, between the particle size distribution and the pore size distribution, which one influences the permeability reduction more? This question will be clarified in the present study.

2. Theoretical Formalisms.

Network Model

In the present study, we use the modified two-dimensional square network to represent the porous media of the filter, and adopt the Brownian dynamic simulation method to track the individual particles as they move through the network (Chang et al., 2004). All pores in the network and particles in the influent are assumed to be with the Raleigh type size distribution (Sharma and Yortsos, 1987). Then, the pore size distribution can be assigned randomly to the bonds in the network as follows,

$$\int_0^{r_1'} 2r'\exp(-r'^2)dr' = 1-\exp(-r_1'^2) \quad (1)$$

with

$$r_1' = \frac{r_f}{r_{mean}} = \sqrt{-\ln(1-a_i)} \qquad (2)$$

and $0 < a_i < 1$

where the random number a_i can be generated by using the standard computer software (IMSL, 1985), r_f and r_{mean} are the radius of filter grains and the mean radius of pores, respectively. And the size distribution of the ith particle in the influent is governed by

$$r_{pi} = r_{pm}\sqrt{-\ln(1-a_i)} \qquad (3)$$

where r_{pm} is the mean radius of particles.

In the current model, two different mechanisms of particle capture are considered: straining (size exclusion) and direct deposition. Straining occurs when the particle diameter is larger than the pore diameter selected for it to transport through the network. Straining plugs up the pore and drops its permeability to zero, and thereby changing the flow direction to other available pores. Direct deposition of a particle on a pore wall occurs as a result of hydrodynamic and DLVO interaction forces acting on the particle (Verwey and Overbeek, 1948). The details of this direct deposition mechanism in a constricted tube cell can be found in Chang et al. (2003).

Constricted Tube Model

We represent the pore geometry in the present network by the constricted tube model (Payatakes et al., 1973). As shown in Fig. 1, the sinusoidal geometric structure (SCT as sinusoidal constricted tube) used by Fedkiw and Newman (1978) is considered for the constricted tube model in the present study. The expressions of the wall radius r_w corresponding to this geometric structures is:

$$r_w = \frac{r_c + r_{\max}}{2}\left[1 + \left(\frac{r_{\max} - r_c}{r_{\max} + r_c}\right)\cos\left(2p\frac{z}{l_f}\right)\right]$$

for $0 < \frac{z}{l_f} < 1$ (4)

In the present study, the flow field equations established by Chow and Soda (1972) and modified by Chiang and Tien (1985) are adopted. The details of these flow field equations can be found in the book of Prof. Tien (1989).

Brownian Dynamics Simulation

Similar to the previous papers by Ramarao et al. (1994) and by authors (Chang and Whang, 1998; Chang, et al., 2003), applying the principle of trajectory analysis, the method of Brownian dynamics simulation is adopted in the present study. With consideration of the inertia term in the force balance equation and of the specification of the flow fluid around the collector, the ith particle position in the tube model can be expressed by the Langevin type equation as (Chang et al., 2004):

$$Z = Z_0 + \left\{\frac{V_0}{b}(1-e^{-bt}) + U\left[t - \frac{1}{b}(1-e^{-bt})\right]\right\}F_1(H)F_2(H)F_3(H) \qquad (5)$$
$$+ \left\{R_r(t) + \left(\frac{F_{LO}+F_{DL}}{bm_p}\right)\left(t + \frac{e^{-bt}}{b} - \frac{1}{b}\right)\right\}F_1(H)F_3(H)$$

with

$$R_r(t) = \int_0^t \left[\int_0^n e^{bz}\, A(z)\, dz\right] e^{-bn}\, dn$$

where $A(t)$ represents a Gaussian white noise process in stochastic terms, b is the friction coefficient per unit mass of particle, and $F_1(H)$, $F_2(H)$, and $F_3(H)$ are the hydrodynamic retardation factors of normal vector, drag force, and shear vector, respectively (Tien, 1989). $R_r(t)$ is the random deviate of position vector with bivariate Gaussian distribution. The detailed formula of $R_r(t)$ can be found in Kanaoka et al. (1983) and Ramarao et al. (1994).

In eq. (5), F_{LO} and F_{DL} are the van der Waals force and the electrostatic repulsion force interacting between the particle and the collector surface, respectively.

$$F_{LO} = -\nabla f_{LO}, \quad F_{DL} = -\nabla f_{DL} \qquad (6)$$

with

$$f_{LO} = -N_{LO}\left[\frac{2(H+1)}{H(H+2)} + \ln H - \ln(H+2)\right]$$

(with the unit of k_BT)

$$f_{DL} = N_{E1}\left\{N_{E2}\ln\left[\frac{1+\exp(-X)}{1-\exp(-X)}\right] + \ln[1-\exp(-2X)]\right\}$$

(with the unit of k_BT)

where $H = \frac{h_s}{r_{pm}}$, $N_{LO} = \frac{A}{6k_B T}$, $N_{DL} = kr_{pm}$,

$X = N_{DL} H$, $N_{E1} = \frac{n r_p (j_1^2 + j_2^2)}{4 k_B T}$,

$N_{E2} = \frac{2\left(\frac{j_1}{j_2}\right)}{\left[1 + \left(\frac{j_1}{j_2}\right)^2\right]}$.

In the above equation, h_s is the smallest separation distance between the particle and the collector surface, A is the Hamaker constant, k_B is the Boltzmann constant, T is the absolute temperature, k is the reciprocal of the electric double layer thickness, n is the dielectric constant of the fluid, and j_1 and j_2 are the surface (zeta) potentials of the particle and the collector, respectively. The algebraic sum of the van der Waals and double-layer potentials gives the total interaction energy curve of the DLVO theory (i.e. $V_T/k_BT = f_{LO} + f_{DL}$) (Verwey and Overbeek, 1948). In this total interaction energy profile, the existence of two characteristic energy barriers (i.e. the height of the primary maximum and the depth of the secondary minimum) is important in determining the permeability reduction K/K_0 (Chang et al., 2004).

The equation used to estimate the change in the local permeability in the ith bond as the function of deposited particles is (Tien, 1989):

$$K_i = \frac{e_i^3 \langle d_f \rangle^2}{180(1-e_i)^2} \qquad (7)$$

where e_i is the local porosity of the ith bond, which will be changed by those particles deposited on the pore walls as the filtration process proceeds. The details of calculating the time-dependent values of e_i and K/K_0 can be found in our previous paper (Chang et al., 2004).

In order to express the extent of permeability reduction as filtration proceeds, we use the permeability ratio K/K_0 as the function of the pore volumes of fluid injected into the filter bed. Here, the pore volume ($p.v.$) of the injection fluid is defined as:

$$p.v. = \frac{U_{in} t}{e_0 L} = \frac{C_{in} V_f}{V_p} \qquad (8)$$

with $V_f = \sum_{i=1}^{N_L} p r_{fi}^2 l_{fi}$ and $V_p = \sum_{i=1}^{N_L} \frac{4}{3} p r_{pi}^3$

where U_{in} is the influent flow rate, C_{in} is the influent number concentration of particles, e_0 is the initial porosity of the filter, L is the length of the filter, r_{fi} is the radius of the ith bond, l_{fi} is the length of periodicity of the ith bond (Tien, 1989), and r_{pi} is the radius of the ith particles.

3. Simulation Results and Discussion

Simulations are performed on a two-dimensional network with $N_L = 70x70$, and the influent velocity is kept at 0.1 cm/sec. The parameter values adopted in the simulation are: e_{i0} = 0.4, r_f =10.0 mm , r_{pm} = 0.5 mm and C_{in} = 1000 particles per cm^3. The effects of two types of interaction energy curves (see Fig. 2) on the permeability ratio will be investigated in the present paper. In order to prove the dominant role of pore size distribution on the reduction of permeability, four different cases of particle and pore size distributions are considered, they are: (1) when particle size and pore size are kept at unique values of r_{pm} and r_f , respectively, (2) particle size with Raleigh type distribution while pore size is kept an unique value of r_f , (3) particle size is kept at an unique value of r_{pm} while pore size with Raleigh type distribution and (4) both particle and pore sizes with Raleigh type distribution.

As shown in Fig. 2, curves A exhibits a large primary maximum and a deep secondary minimum, while a "barrierless" type interaction energy curve is represented

by curve B. In this figure, N_{E1}=105.0 and N_{DL}=10.75 for curve A, N_{E1}=0.0 and N_{DL}=0.0 for curve B, and N_{E2}=1.0 and N_{L0}=7.0 for all two curves. Our previous paper (Chang et al., 2003) calculated the collection efficiencies of particles in SCT, and found that the collection efficiency of curve B is always greater than that of curve A when Reynolds number of fluid is small because there is no energy barrier exists, and the deposition mechanism of particles is controlled by the Brownian diffusion effect. For curve A, it was found that, even with the presence of the deep secondary minimum which increases the accumulation probability of particles, the steep slope between the secondary minimum and the primary maximum energy barriers (i.e. a repulsive force) observed in this curve is the main reason for its low collection efficiency (Chang et al., 2003). Corresponding to curves A and B in Fig. 2, the simulation results of the permeability ratio as the function of pore volumes injected are given in Fig. 3 and Fig. 4 as follows, respectively.

As shown in Fig. 3, we can find that the permeability ratio decreases with the increase of pore volumes injected for all of four cases considered in the present paper. Because of the existed repulsive energy barrier of curve A and the Brownian diffusion effect are unfavorable for the particles to deposit at the inlet region of the filter, hence those Brownian particles can transport further inside the network and increase the probability of straining small pores. Since the large size part of particles has greatest probability to plug those small size part of pores, therefore the case of both particle and pore sizes with Raleigh type distribution can cause the highest permeability reduction among those four cases considered in Fig. 3. When comparing the initial decreasing rates of those four curves shown in Fig. 3, because bigger particles have greater probability of straining those smaller pores in the relative size distributions, we can find that straining is the main mechanism to reduce the permeability at the initial period of injection for the case of Raleigh distribution, and vice versa for the case of constant size value where the direct deposition mechanism becomes dominant. Also, in this figure, we can find that the two cases of pore size with Raleigh distribution always cause a lower permeability ratio than those two cases of pore size kept at constant values, which indicates that the pore size distribution is more dominant in reducing the permeability than that of the particle size distribution in the present study, especially at the initial period of filtration.

Corresponding to the "barrierless" curve B shown in Fig. 2, the relationships between the permeability ratio and the pore volumes injected are shown in Fig. 4. Similar to those obtained in Fig. 3, the permeability ratio for the case of both particle and pore sizes with Raleigh type distribution is the lowest among those four considered cases, and the permeability ratios for the two cases of pore size with Raleigh distribution are always lower than those two cases where the pore size is kept at the constant value. Therefore, the pore size distribution and the straining mechanism still dominate the reduction of permeability for this "barrierless" curve B. Comparing those values of K/K_0 between Fig. 3 and Fig. 4, since the existed unfavorable deposition energy barrier will drive more particles deeper inside the network to plug more small pores (i.e. straining), hence the permeability ratios of curve A are lower than those of Curve B when those pore sizes with Raleigh type distribution. But, for the case of those pores with Raleigh distribution and particles with an unique value where the direct deposition mechanism becomes dominant, the permeability ratios of curve A are higher than those of Curve B. For the case of both pores and particles with an unique value, the permeability ratios of curve A are almost the same as those of Curve B.

In our previous paper (Chen et al., 2003), with the use of the orthogonal collocation principle and the pseudo-spectral method based on the Chebyshev polynomial, we successfully solved the conventional transport equations describing the deposited particles, the suspended particles and the un-plugged pores in the porous media for the different network structures (i.e. the Lagrangian type approach). In that paper, by assuming all pore sizes are with the Raleigh type distribution (same as the present paper), we found that small pores at the

entrance region of filter bed are easier plugged by those deposited particles (i.e. straining) than those large pores at the initial period of filtration, even those large pores are retaining most fraction of influent particles when the breakthrough moment is achieved. This result is similar with the conclusion obtained in the present simulation work; the pore size distribution has more profound effect on reducing the permeability than that of the particle size distribution, especially at the initial period of filtration.

References:

Chang, Y. I., & Whang, J. J. (1998). Deposition of Brownian particles in the presence of energy barriers of DLVO theory: effect of the dimensionless groups. *Chemical Engineering Science*, 53(23), 3923-3939.

Chang, Y. I., Chen, S. C., & Lee, E. (2003). Prediction of Brownian particle deposition in porous media using the constricted tube model. *J. Colloid Interface Sci*., 266(1), 48-59.

Chen, S. C., Lee, E., & Chang, Y. I. (2003). Effect of the coordination number of the pore-network on the transport and deposition of particles in porous media. *Separation and Purification Technology*, 30 (1), 11-26.

Chang, Y. I., Chen S. C., Chan H. C., & Lee, E. (2004). Network Simulation for Deep Bed Filtration of Brownian Particles. *Chemical Engineering Science*, 59 (21), 4467-4479.

Chiang, H. W., & Tien, C. (1985). Dynamics of deep-bed filtration: Part I. Analysis of two limiting situations. *A.I.Ch.E. J.*, 31(8), 1349-1359.

Chow, J. C. F., & Soda, K. (1972). Laminar flow in tubes with constriction. *Phys. Fluids*, 15(10), 1701-1706.

Fedkiw, P., & Newman, J. (1977). Mass transfer at high Peclet number for creeping flow in a packed-bed reactor. *A.I.Ch.E. J.*, 23(3), 255-263.

Herzig, J. P., Leclerc, D. M., & LeGoff, P. (1970). Flow of suspension through porous media – application in deep bed filtration. *Ind. Engng. Chem.* 62(1), 8-35.

Imdakm, A. O., & Sahimi, M. (1991). Computer simulation of particle transport processes in flow through porous media. *Chemical Engineering Science*, 46(8), 1977-1993.

IMSL Libraries, IMSL (1985), Houston, Texas.

Ison, C. R., & Ives, K. J. (1969). Removal mechanisms in deep bed filtration. *Chemical Engineering Science*, 24(2), 717-729.

Kanaoka, C., Emi, H., & Tarthapanichakoon, W. (1983). Convective diffusional deposition and collection efficiency of aerosol on a dust-loaded fiber. *A.I.Ch.E. J.*, 29(6), 895-902.

Kim, J. S., & Rajagopalan, R. (1982). A comprehensive equation for the rate of deposition of colloidal particles and for stability ratios. *Colloids Surfaces*, 4(1), 17-31.

Kirkpatrick, S. (1973). Percolation and conduction. *Rev. Mod. Phys.*, 45(4), 574-588.

Payatakes, A. C., Tien, C., & Turian, R. M. (1973). A new model for granular porous media: Part I. Model formulation. *A.I.Ch.E. J.*, 19(1), 58-67.

Ramarao, B. V., Tien, C. & Mohan, S. (1994). Calculation of single fiber efficiencies for interception and impaction with superposed Brownian motion. *J. Aerosol Sci*., 25(2), 295-313.

Rege, S. D., & Fogler H. S. (1988). A network model for deep bed filtration of solid particles and emulsion drops. *A.I.Ch.E. J.*, 34(11), 1761-1772.

Sharma, M. M., & Yortsos, Y. C. (1987). A network model for deep bed filtration processes. *A.I.Ch.E. J.*, 33(10), 1644-1653.

Soo, H., & Radke, C. J. (1984). The flow mechanism of dilute, stable emulsions in porous media. *Ind. Eng. Chem. Funda.*, 23(3), 342-347.

Tien, C., & Payatakes, A. C. (1979). Advances in deep bed filtration. *A.I.Ch.E. J*., 25(5), 737-759.

Tien, C. (1989). *Granular filtration of aerosols and hydrosols.* Chapters 3, 4 and 5. Boston: Butterworhts.

Verwey, E. J. W., & Overbeek, J. Th. G. (1948). *Theory of the stability of lyophobic colloids.* Amsterdam: Elsevier.

Yao, K. M., Habidian, M. T., & O'Melia, C. R. (1971). Water and waste water filtration: concepts and applications. *Environ. Sci. Technol*., 5(11), 1105-1116.

Legend of Figures

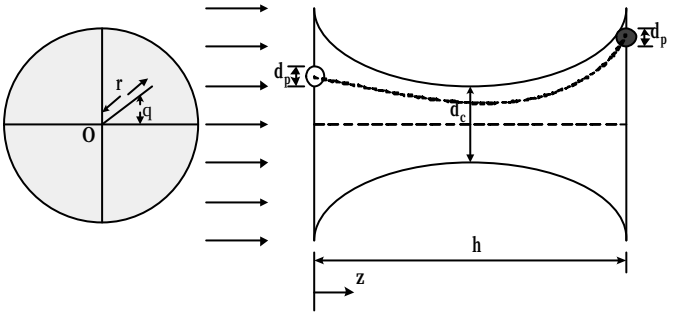

Figure 1. The schematic diagram of the constricted tube model.

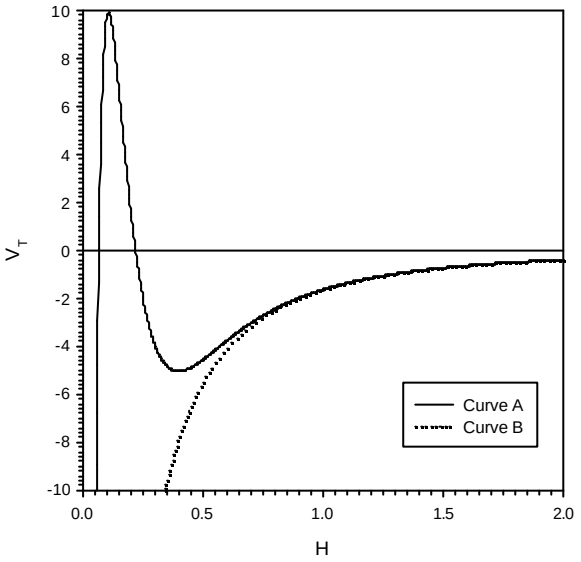

Figure 2. Two types of total interaction energy curves adopted in the simulation of the present paper, at which N_{E1}=105.0 and N_{DL}=10.75 for curve A, N_{E1}=0.0 and N_{DL}=0.0 for curve B, and N_{E2}=1.0 and N_{L0}=7.0 for all two curves.

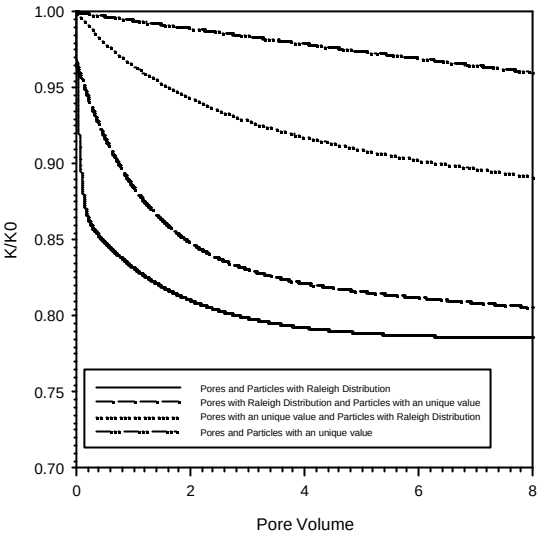

Figure 3. Effect of both particle and pore size distributions on the permeability ratio K/K_0 as the function of pore volumes injected, corresponding to curve A shown in Fig. 2.

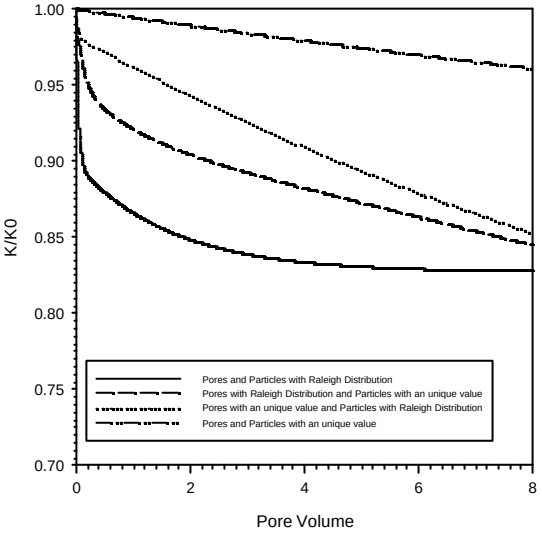

Figure 4. Effect of both particle and pore size distributions on the permeability ratio K/K_0 as the function of pore volumes injected, corresponding to curve B shown in Fig. 2.